

Ballistic Motion in Quenched Random Environments

Sune Jespersen^{a*} and Hans C. Fogedby^{a,b}

^aInstitute of Physics and Astronomy, University of Aarhus, 8000 Århus C, Denmark,

^bNORDITA, Blegdamsvej 17, 2100 København Ø, Denmark

November 12, 2018

Abstract

We study the motion of a massive particle in a quenched random environment at zero temperature. The distribution of particle positions is investigated numerically and special focus is placed on the mean stopping distance and its fluctuations. We apply a scaling analysis in order to obtain analytical information about the distribution function. The model serves as a simple example of transport in a random medium.

PACS numbers: 36.20.-r, 47.55.-t, 05.60.-k

Keywords: random environments; pinning; scaling analysis; stretched exponentials; non-gaussian

*Corresponding author. Address as above. Email: sune@ifa.au.dk. Telephone (+45) 89423680, fax (+45) 86120740.

distributions.

1 Introduction

Dynamics in random media constitute a set of phenomena widely studied in modern statistical physics and soft condensed matter. The problems in questions extend from the growth of interfaces to the diffusion of scalars in disordered materials [1–6]. In order to understand the motion of manifolds in random environments with focus on the pinning mechanism, thermal fluctuations are to a first approximation often disregarded, see e.g., [7–9]. A particular simple case is the motion of a massive particle, i.e., a zero dimensional manifold, in a random medium subject to pinning.

This model was recently analyzed by Stepanow and Schulz [10]. They studied the behavior of a Newtonian particle of mass m in a random environment in d -dimensions described by the equation of motion $m\ddot{\mathbf{x}} = \mathbf{F}(\mathbf{x})$; here \mathbf{F} is a quenched random force with a Gaussian distribution of strength σ . In dimensions d larger than one, the large time results of Stepanow and Schulz for the first two cumulants are given by

$$\langle \mathbf{x} \rangle_F \propto \frac{v_0^4 m^2}{\sigma(d-1)} \hat{\mathbf{v}}_0 \quad \text{and} \quad \langle (\mathbf{x} - \langle \mathbf{x} \rangle_F)^2 \rangle_F \propto t \frac{v_0^5 m^2 d}{\sigma d(d-1)}. \quad (1)$$

Here $\hat{\mathbf{v}}_0$ denotes a unit vector along the direction of the initial velocity \mathbf{v}_0 . In one dimension the results in Eq. (1) are undefined owing to the diverging denominators. This behavior reflects the fact that in one dimension the force $F(x)$ can always be derived from a potential. The energy is thus

conserved in this model and the particle will simply oscillate back and forth between two potential barriers.

In the present paper we extend the results of Stepanow and Schulz[10] by including a friction term in the equation of motion and thus allowing for random pinning in the one dimensional case. The paper is organized as follows. In Section 2 we define the model and write down the appropriate equations of motion both on the level of the stochastic equation of motion and the associated Kramers equation for the time dependent distribution. In Section 3 we outline the numerical analysis applied to the equation of motion. In Section 4 we carry out a simple scaling analysis, identifying the relevant parameters and the scaling functions describing the two first cumulants of the stationary distribution. Section 5 deals with the numerical results and we close the paper with a summary and conclusion in Section 6.

2 The Model

In one dimension the motion of a particle of mass m moving in a viscous medium and subject to a random force field $F(x)$, depending on the actual position x of the particle, is governed by the Langevin equation

$$m \frac{d^2x}{dt^2} + \gamma \frac{dx}{dt} = F(x) + \eta(t) . \quad (2)$$

Here γ is the coefficient of friction and $\eta(t)$ a thermal Gaussian white noise with correlations $\overline{\eta(t)\eta(t')} = 2D\delta(t - t')$. The noise strength D is given by the fluctuation-dissipation theorem, $D = \gamma k_B T$; T is the temperature of the medium. The distribution of F is also chosen to be Gaussian with the correlations

$$\langle F(x) \rangle = 0 \quad \text{and} \quad \langle F(x)F(x') \rangle = \sigma\delta(x - x') ; \quad (3)$$

here σ is the force correlation strength.

In the present context we consider the case where the random trapping dominates the physics and we shall thus disregard the thermal fluctuations relative to the random environment characterized by F , that is we set $D = 0$ in Eq. (2); this limit corresponds to zero temperature or to a very massive particle $m \rightarrow \infty$. Breaking up Eq. (2) it can then also be written as the set of equations

$$\frac{dv}{dt} = -\gamma v + F(x) , \quad (4)$$

$$\frac{dx}{dt} = v , \quad (5)$$

where we for convenience have set $m = 1$. Equivalently, we can also choose to discuss the problem in terms of an equation for the distribution function $P(x, v, t)$ itself, namely the Kramers equation in the limit of zero diffusion coefficient [11]:

$$\frac{\partial P(x, v, t)}{\partial t} = \left[\frac{\partial}{\partial v} (v\gamma - F(x)) - v \frac{\partial}{\partial x} \right] P(x, v, t) . \quad (6)$$

As earlier stated, in the limit $\gamma = 0$ the model described by Eqs. (5)-(6) above reduces to the

one discussed by Stepanow and Schulz in [10]. However, here we allow for dissipation by having a non-zero γ , and entirely different physics will arise.

3 Discretization and Numerical Accuracy

In order to render the problem amenable to numerical analysis we modify the force correlations Eq. (3) defined on the continuum by applying a finite width a_0 to the delta function (or equivalently, formulating the problem on a lattice) in such a manner that

$$\langle F(x)F(x') \rangle = (\sigma/a_0) \delta_{n(x),n(x')} . \quad (7)$$

The subscript $n(x)$ of the Kronecker delta in Eq. (7) is thus a counter of which cell in the lattice the position x refers to; more precisely, $n(x) = \{n \in \mathbb{Z} \mid x \in [na_0; (n+1)a_0]\}$. In the limit $a_0 \rightarrow 0$ we recover the full continuum description in Eq. (3).

The equations of motion in Eq. (5) are solved numerically by means of the fourth order Runge–Kutta method (RK4) [12]. First, by calling a random generator an actual realization of the force field is generated corresponding to a specific environment. In the next step we solve the equations of motion with the specific initial conditions that the particle initiates its path at $x = 0$ at $t = 0$ with initial velocity v_0 . A typical trajectory originating from a simulation is shown in Fig. 1 below. Finally, we perform an average over realizations of the force field, typically of the order of 10000 realizations.

There are three different sources of uncertainty in the simulations: The finite time step τ , the finite lattice distance a_0 , and the finite number of samples of the random force distribution. Moreover, they are not independent: Decreasing a_0 will require a smaller τ in order to keep the error small, since a smaller lattice constant leads to a more erratic potential in which the numerical solution is more sensitive to the magnitude of τ . Choosing a value for a_0 we fix τ such that the stopping distance of the particle in a specific environment does not change more than a prescribed fraction (numerical precision) when decreasing τ by a factor of say 10. Then we sample a large number of realizations of the environment such that the statistical errors are below the desired precision. The typical relative numerical error in the simulations is about 1%, and the typical relative statistical error is no more than 5%.

4 Scaling Analysis

Before we embark on a more detailed discussion of the numerical results it is illuminating to perform a simple scaling analysis. Rescaling space and time in an affine manner according to $x \rightarrow xb = \tilde{x}$ and $t \rightarrow at = \tilde{t}$, where a and b are scale parameters to be determined, the velocity scales like $v \rightarrow vb/a = \tilde{v}$ and we obtain by insertion in Eq. (5) the scaled equation of motion $d\tilde{v}/d\tilde{t} = bF(x)F(x)/a^2 - (\gamma/a)\tilde{v}$. The force on the rescaled lattice is thus given by $\tilde{F}(\tilde{x}) = bF(x)a^2$, is also Gaussian and correlated according to $\langle \tilde{F}(\tilde{x})\tilde{F}(\tilde{x}') \rangle = b^3/a^4\sigma\delta(\tilde{x} - \tilde{x}')$. Concluding, we infer the following scaling of the

parameters: $\sigma \rightarrow \tilde{\sigma} = \sigma b^3/a^4$, $\gamma \rightarrow \tilde{\gamma} = \gamma/a$, $v_0 \rightarrow \tilde{v}_0 = (b/a)v_0$, and $a_0 \rightarrow \tilde{a}_0 = ba_0$. Choosing the scale factors a and b in such a manner as to eliminate the dependence on the force strength σ and the friction coefficient γ , i.e., $a = \gamma$ and $b = \gamma^{4/3}/\sigma^{1/3}$, we finally obtain the scaling form

$$x(t) = \frac{\sigma^{1/3}}{\gamma^{4/3}} G_1 \left(\gamma t, v_0(\gamma/\sigma)^{1/3}, a_0(\gamma^4/\sigma)^{1/3} \right) , \quad (8)$$

where G_1 is a random function depending on the actual force realization. The above scaling analysis can, of course, also be carried out on the basis of the Kramers equation Eq. (6).

In the following we limit our discussion to the statistical properties of the final position of the particle. In this limit the dependence on time disappears and we obtain

$$x \equiv x(\infty) = \frac{\sigma^{1/3}}{\gamma^{4/3}} G \left(v_0 (\gamma/\sigma)^{1/3}, a_0 (\gamma^4/\sigma)^{1/3} \right) , \quad (9)$$

where G is a new scaling function. The physical meaning of the first argument in the scaling function G is related to energy considerations. In one dimension the force F derives from a potential U according to $U(x) = - \int_0^x F(x') dx'$ and, correspondingly, the mean square fluctuation of U is given by $\langle U^2(x) \rangle = \int_0^x dx' \int_0^x dx'' \langle F(x') F(x'') \rangle = \sigma x$. Consequently, the typical potential energy of the disorder behaves as $\sqrt{\sigma x}$; this also follows from the fact that the potential performs a ‘random walk’ in x -space. Evaluating this energy at the trapped position of a free particle, i.e., v_0/γ , we obtain a typical upper limit for the pinning energy. Comparing this energy to the initial energy of a free particle, $\sim v_0^2$, we arrive at the following parameter characterizing the degree of disorder:

$$\mu = \frac{E_{\text{free}}}{E_{\text{disorder}}} \sim \left(v_0 \left(\frac{\gamma}{\sigma} \right)^{1/3} \right)^{3/2} , \quad (10)$$

i.e., a power of the first argument in the scaling function. Here small values of the dimensionless parameter μ corresponds to *strong* disorder, whereas large values of μ characterizes *weak* disorder.

5 Analysis of Numerical Data

In this section we study the various moments of the variable $x = x(\infty)$ as a function of the initial velocity v_0 and the disorder strength σ . Numerical accuracy and the associated computation time puts a limit to the range of values for which we examine the scaling function G . We have in particular analyzed the weak disorder regime determined by $10 \lesssim \mu \lesssim 100$. Stronger disorder requires better routines or much longer computation time in order to acquire the same accuracy.

5.1 The trajectory

It is instructive first to consider the outcome of a typical simulation. In Fig. 1 we have thus shown a simulated trajectory with a superposed trajectory of the free flight, corresponding to the solution of Eq. (5) with $F(x) = 0$, i.e.,

$$x_{\text{free}}(t) = \frac{v_0}{\gamma} (1 - \exp(-\gamma t)) , \quad (11)$$

with $x(0) = 0$ and $v(0) = v_0$.

The initial motion follows that of a free particle, however, as the kinetic energy degrades due to friction the particle will soon experience a (random) force large enough to reverse the motion.

In order to illustrate this effect we depict Fig. 2.a the potential energy $U(x)$ (solid curve) and the kinetic energy of free flight (the dashed curve) a function of position. The point of intersection of the two curves is to a first approximation the point of first reflection of the particle. The actual motion of the particle is, of course, sensitive to the disorder before the point of reflection, perturbing the dashed curve on the figure. After the first reflection the velocity is reversed and the process reiterates. Owing to the gradual loss of kinetic energy the particle travels shorter and shorter distances and finally comes to rest in a local minimum of the potential. Figure 2.b is a magnification of the region around the minimum that finally traps the particle.

In Fig. 3.a we show the distribution of final positions and note the general trend that the particle travels shorter than for the corresponding free motion. This is illustrated by the vertical line on the figure, indicating the final position for a free particle with the same initial velocity. Despite a superficial resemblance the distribution depicted in Fig. 3.a is not Gaussian. A transparent way to exhibit this deviation from Gaussian behavior is to plot the logarithm of the distribution; a Gaussian distribution then yields a parabolic shape. This plot is shown in Fig. 3.b, where we have also included a fit to a parabola. It follows from the fit that the actual distribution possesses long tails.

5.2 Mean distance traveled

A central quantity is the total mean distance traveled by a particle, $\langle x \rangle_F$, as a function of the initial velocity v_0 and the force correlation strength σ . The notation $\langle \cdot \rangle_F$ here denotes an average over the

Gaussian force distributions. In Fig. 4 we have depicted $\langle x \rangle_F$ as a function of σ for fixed damping $\gamma = 5.0$ and initial velocity $v_0 = 10.0$. Data from two different seeds, i.e., two series of realizations of the random force field, are shown in order to indicate the statistical uncertainty.

The data are reasonably independent of the small distance cutoff a_0 , and thus applying the scaling form Eq. (9) we infer

$$\langle x \rangle_F = \frac{\sigma^{1/3}}{\gamma^{4/3}} \langle G(v_0(\gamma/\sigma)^{1/3}) \rangle_F . \quad (12)$$

A good fit to the data in Fig. 4 is provided by the stretched exponential $\langle x \rangle_F \sim a \exp(-b\sigma^c)$. Averaging over a set of data with different cutoffs a_0 in the range from 0.01 to 0.001 we obtain for the parameters $a = 2.000 \pm 0.001$, $b = 0.058 \pm 0.001$, and $c = 0.34 \pm 0.01$. The error bars are extracted from an appropriate sample of data. The data are thus consistent with the scaling form

$$\langle x \rangle_F \sim \frac{v_0}{\gamma} \exp\left(-\frac{(\sigma/\gamma)^{1/3}}{v_0}\right) , \quad (13)$$

which has the correct limiting form $x \sim v_0/\gamma$ in the absence of disorder or large initial velocity v_0 . Also, in the limit of vanishing friction $\gamma \rightarrow 0$ the first moment $\langle x \rangle_F$ vanishes. Consequently, there is a largest mean distance traveled for an appropriately selected value of the friction. Since we are here considering the weak disorder regime one could argue that the first two terms in the expansion of the stretched exponential are sufficient. We shall however stick to the expression in Eq. (13) since it behaves correctly in the limit $\gamma \rightarrow 0$.

As an alternative check of the scaling form Eq. (13) we next vary the initial velocity v_0 . The data

are shown in Fig. 5 for the values $\gamma = 5.0$ and $\sigma = 1.0$. It follows that Eq. (13) does describe the data well. Also shown is a linear fit and a fit to a stretched exponential. We note that all curves appear to coincide on the figure, thus not allowing us to distinguish the best fit.

5.3 Fluctuations in the stopping distance

The last issue we address is the root mean square fluctuations of the stopping distance $\Delta x = \sqrt{\langle (x - \langle x \rangle)^2 \rangle}$, depicted in Fig. 3. Here the situation is a little complicated since we find a dependence on the small distance cutoff a_0 . From the general scaling analysis yielding Eq. (9) we infer a scaling form for Δx ,

$$\Delta x = \sqrt{\langle (x - \langle x \rangle)^2 \rangle} = \frac{\sigma^{1/3}}{\gamma^{4/3}} G_2(v_0(\gamma/\sigma)^{1/3}, a_0(\gamma^4/\sigma)^{1/3}) , \quad (14)$$

where G_2 is a new unknown scaling function.

In Fig. 6 we have for fixed damping $\gamma = 5.0$ and initial velocity $v_0 = 10.0$ plotted the standard deviation of x versus the disorder strength σ for two different cutoffs a_0 on a log-log scale. The linear fit suggests the simple power law behavior

$$\Delta x = u_1 \sigma^{z_1} . \quad (15)$$

In order to determine the dependence on the lattice constant a_0 we have in Figs. 7 and 8 plotted the exponent z_1 and the amplitude u_1 as a function of a_0 in order to study the limiting function $G_2(v_0(\gamma/\sigma)^{1/3}) = \lim_{a_0 \rightarrow 0} G_2(v_0(\gamma/\sigma)^{1/3}, a_0(\gamma^4/\sigma)^{1/3})$ for decreasing a_0 . With a linear fit we find the

following values for the amplitude and the exponent:

$$u_1 = 0.143 \pm 0.001, \quad z_1 = 0.326 \pm 0.002, \quad (16)$$

indicating that the best fit is obtained using a constant scaling function $G_2 = \text{const.}$. We are thus led to the form

$$\Delta x = \text{const.} \frac{\sigma^{1/3}}{\gamma^{4/3}}, \quad (17)$$

independent of initial velocity. Substantiating our result we have finally in Fig. 9 plotted Δx versus v_0 . The independence of Δx on v_0 is quite convincing.

6 Summary and Conclusions

In this paper we have studied a simple model for damped ballistic transport in a random environment: A massive particle moving in a random medium also subject to a viscous force. From energy considerations alone it is clear that the particle will eventually become pinned at a local minimum of the potential and we have thus restricted our attention to the properties of the stationary distribution. We performed an elementary scaling analysis of the equation of motion and exploited the results in the ensuing numerical analysis. Here we restricted our attention to the behavior of the first two cumulants, i.e. the mean stopping distance and the mean square fluctuations of the stopping distance as functions of disorder strength and initial velocity. We found that the data in the weak

disorder regime were well described by the expressions:

$$\langle x \rangle_F \sim \frac{v_0}{\gamma} \exp \left(-\frac{(\sigma/\gamma)^{1/3}}{v_0} \right), \quad \langle (x - \langle x \rangle)^2 \rangle^{1/2} \sim \text{const.} \frac{\sigma^{1/3}}{\gamma^{4/3}}. \quad (18)$$

We, moreover, exhibited the non-Gaussian nature of the stationary distribution of stopping positions of the particle.

There are many more quantities of interest that one could extract numerically. First of all it would be interesting to explore also the dynamic properties, that is the behavior of e.g. $x(t)$ and $v(t)$. Moreover, a more thorough analytical examination would also be desirable. Finally, an extension of the model to the case of a random force with a non-vanishing mean value would introduce some new facets into the problem.

References

- [1] Ya. G. Sinai, Theory Prob. Appl. **27**, 256 (1982). For a review see [2] and [3].
- [2] J.-P. Bouchaud and A. Georges, Phys. Rep. **195**, 127 (1990).
- [3] J.-P. Bouchaud, A. Comtet and A. Georges, Ann. Phys. **201**, 285 (1990).
- [4] R. Bruinsma and G. Aeppli, Phys. Rev. Lett. **52**, 1547 (1984).
- [5] J. Koplik and H. Levine, Phys. Rev. B **32**, 280 (1985).

- [6] P. G. de Gennes, Rev. Mod. Phys. **57**, 827 (1985).
- [7] O. Narayan and D. S. Fisher, Phys. Rev. B. **49**, 9469 (1994)
- [8] D. S. Fisher, Phys. Rep. **301** 113 (1998).
- [9] M. Kardar, Phys. Rep. **301** 112 (1998).
- [10] S. Stepanow and M. Schulz, Physica A **189**,22 (1992).
- [11] H. Risken, *The Fokker–Planck Equation*, Springer–Verlag, Berlin Heidelberg 1989.
- [12] W. H. Press and S. A. Teukolsky and W. T. Vetterling and B. P. Flannery, *Numerical Recipes in C*, Cambridge University Press, New York 1992.

Figures

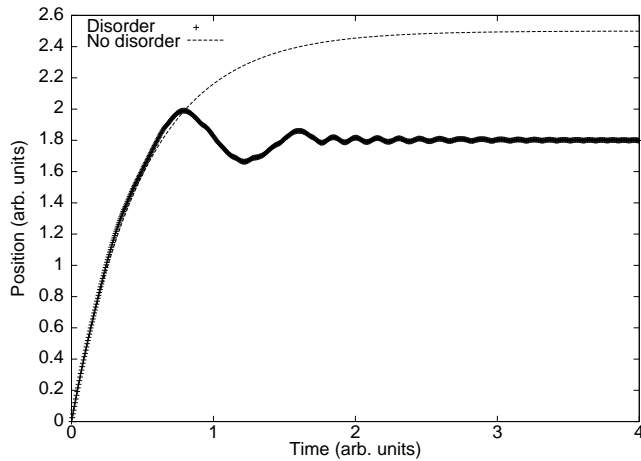


Figure 1: We show a typical trajectory of ballistic motion in one dimension in a random force field (the full line). For comparison we also depict the trajectory of the motion in the absence of disorder (the dashed line). Notice how the trajectories are very similar at short times, whereas for larger times they differ substantially.

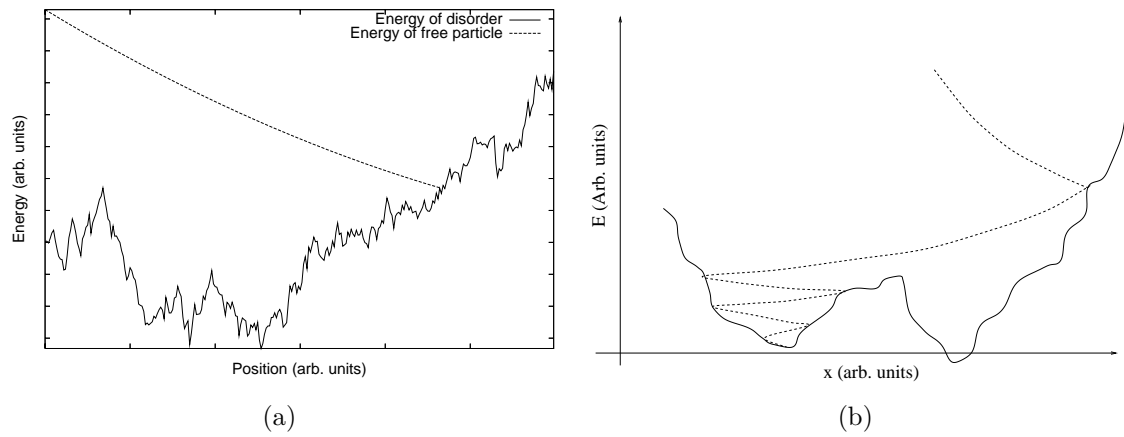


Figure 2: (a): Comparison of the typical energy of the disorder, which is a random walk in x -space, with the energy of the free particle, as a function of position. (b): The particle reflects a number of times on the potential and gradually loses its energy, until it is trapped in a local minimum of the potential.

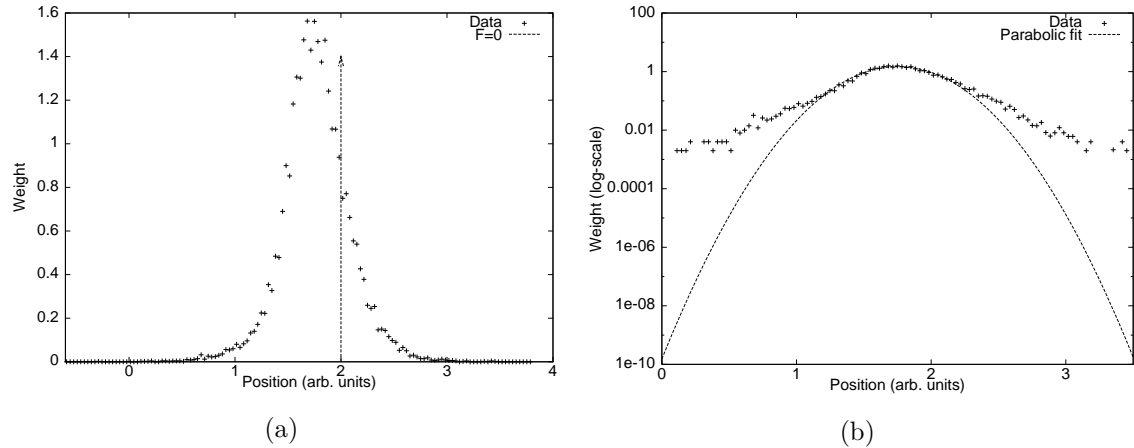


Figure 3: In (a), we plot the stationary distribution of the particles rest position. The vertical line at $x = 2$ marks the final position of a free particle having the same initial velocity. In (b) we have shown the same data on a semi log scale. A fit to a parabola is also shown, and the deviation from Gaussian behavior is seen to be large especially away from the center.

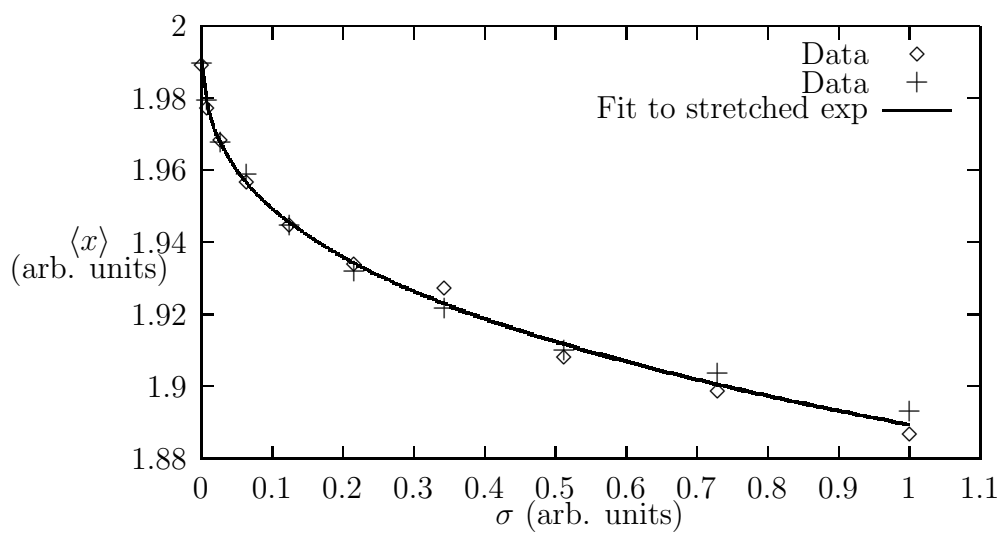


Figure 4: The mean stopping distance as a function of disorder strength σ . The data (from both seeds) have been fitted to a stretched exponential (solid line).

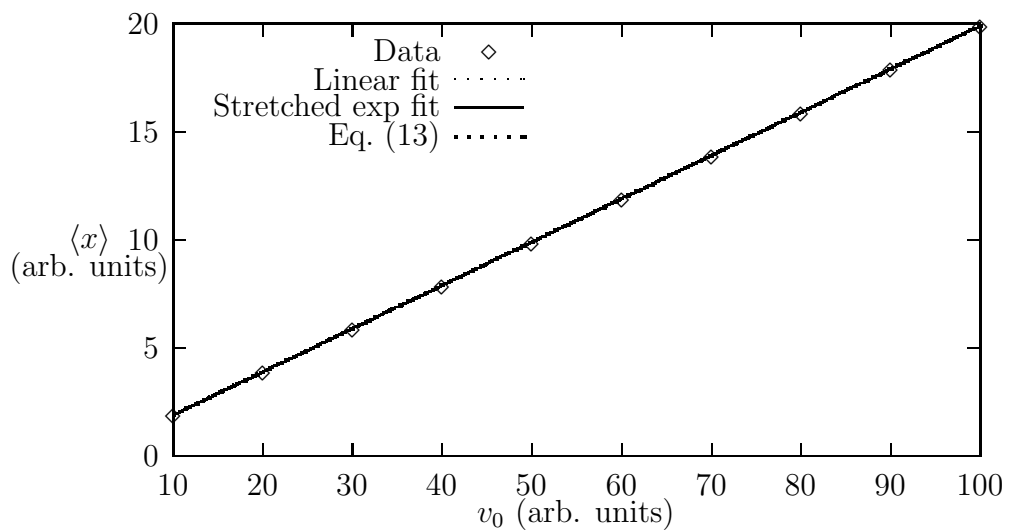


Figure 5: This is a plot of $\langle x \rangle$ versus v_0 . We have shown both a linear fit, a fit to a stretched exponential, and also the prediction Eq. (13). They are all indistinguishable in this plot.

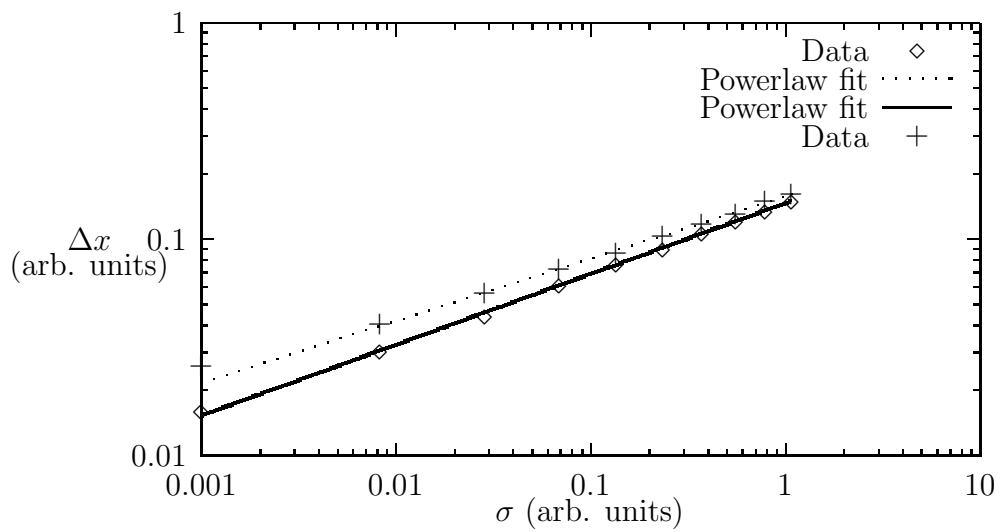


Figure 6: A graph of standard deviation Δx of stopping distribution as a function of strength of disorder. The two different sets of data are for two different lattice constants. The straight lines indicate power-law behavior, albeit with different exponents and amplitudes.

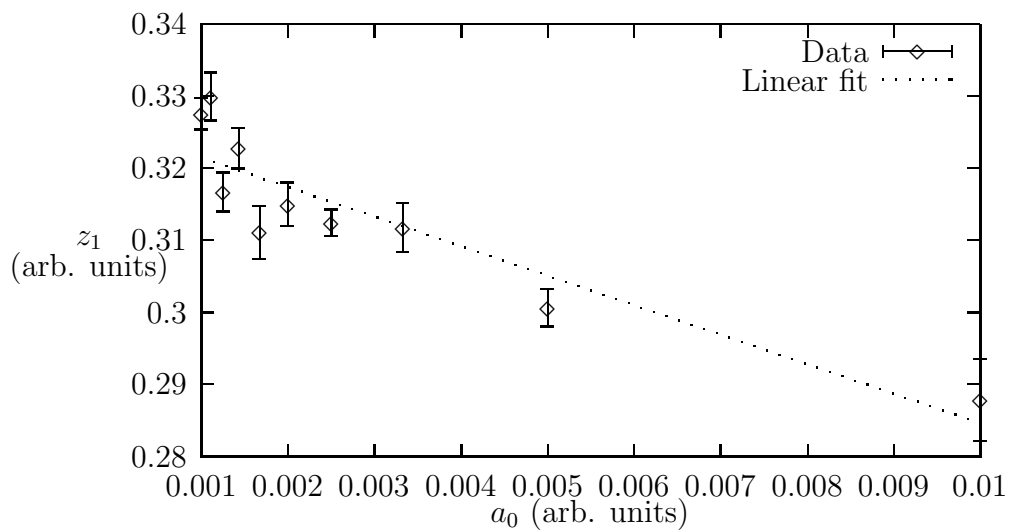


Figure 7: Exponent z_1 (see Eq. (15) of the power law fits as a function of the lattice constant, and a fit to a straight line. We are interested in the limit $a_0 \rightarrow 0$.

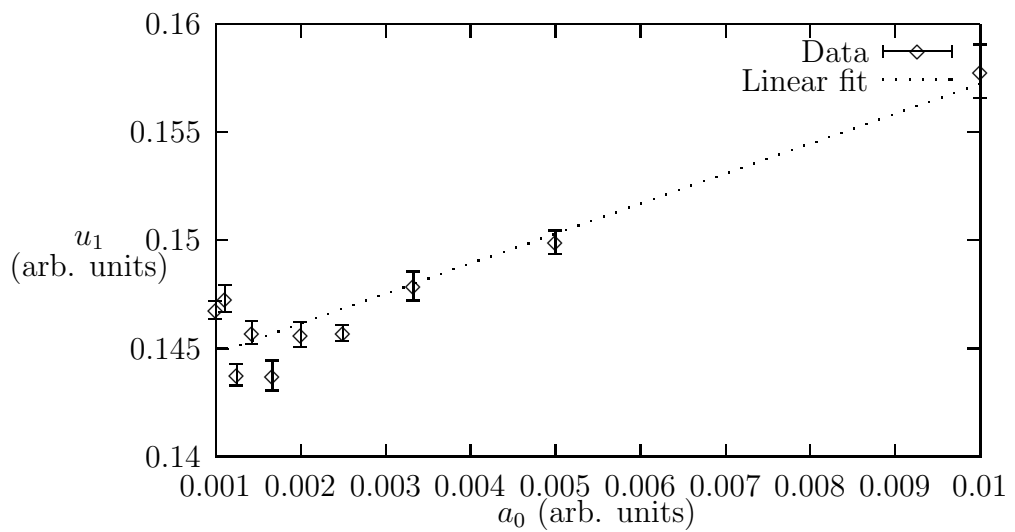


Figure 8: Amplitude u_1 in Eq. (15) of the power law fits as a function of the lattice constant, and a fit to a straight line.

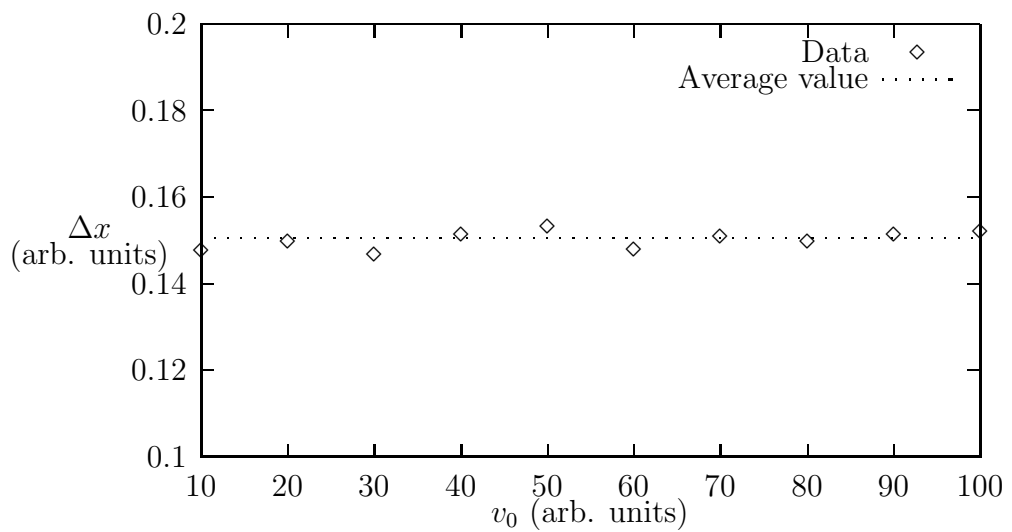


Figure 9: The dependence of the width of stopping distances on the initial speed v_0 is seen to be well approximated by a constant expression. From this figure we have $\Delta x = 0.154$.